INTERNATIONAL JOURNAL OF HYDROGEN ENERGY 37 (2012) 7554–7564

Available online at www.sciencedirect.com

SciVerse ScienceDirect

journal homepage: www.elsevier.com/locate/he

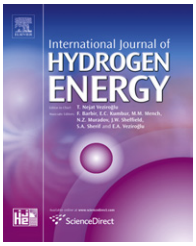

Production of hydrogen-rich fuels for pre-combustion carbon capture in power plants: A thermodynamic assessment

Fontina Petrakopoulou [a,b,*], *George Tsatsaronis* [a]

[a] *Technische Universität Berlin, Marchstr. 18, 10587 Berlin, Germany*
[b] *IMDEA Energy Institute, c/Tulipán s/n, 28933 Mostoles, Madrid, Spain*

ARTICLE INFO

Article history:
Received 21 October 2011
Received in revised form
23 January 2012
Accepted 28 January 2012
Available online 6 March 2012

Keywords:
Hydrogen production
Exergetic analysis
Pre-combustion CO_2 capture
Combined-cycle power plant
Methane steam reforming
Autothermal reforming

ABSTRACT

Hydrogen-fueled plants can play an important role in the field of carbon capture and storage, because they facilitate the mitigation of harmful emissions. In this paper, two combined-cycle power plants with pre-combustion CO_2 capture are examined, in which natural gas is converted into a hydrogen-rich fuel through reforming. The first plant considered operates with a hydrogen-separating membrane and the second with an autothermal reformer. The two plants are compared to a reference plant without CO_2 capture and briefly to alternative oxy-fuel and post-combustion capture technologies. It is found that both plants suffer high penalties caused by the high energy requirements of the reforming components and the CO_2 compression units. Additionally, both plants appear inferior to alternative capture technologies. When comparing the two reforming plants, the plant with the hydrogen-separating membrane operates somewhat more efficiently. However, in order to make these technologies more attractive, their thermodynamic efficiency must be enhanced. The potential for improving the efficiencies of these plants is revealed by an exergetic analysis.

1. Introduction

Hydrogen is an energy carrier that does not generate greenhouse gases when combusted. Due to this trait, hydrogen has attracted attention as a potential alternative to fossil fuels for high efficiency and minimization of harmful exhausts. Hydrogen can be produced from fossil fuels and water using various technologies [1]. Fossil-fuel conversion technologies for the production of hydrogen are well developed and can be used in large scale in the short term. Specifically, gasification (e.g., [2,3]) methane steam reforming (e.g., [4–6]) and partial oxidation (e.g. [7,8]) have been widely studied as potential alternatives to producing hydrogen-rich fuels with promising results. Gasification is one of the best known ways to produce a hydrogen-containing gas from solid fuels (e.g., coal and biomass) that can then be used, in integrated gasification-combined-cycle (IGCC) power plants [2]. Although some IGCC plants have already been constructed, economic and reliability issues delay the wider implementation of the technology. In addition to the concept of gasification, methane steam reforming and partial oxidation are suggested as alternative means to produce hydrogen from natural gas.

Carbon capture and storage is a way suggested to mitigate emissions generated from the combustion of fossil fuels [9]. Carbon capture methods can be separated into three groups: post-combustion, oxy-fuel combustion and pre-combustion [10]. Pre-combustion methods involve the conversion of a carbon-based fuel into a clean, hydrogen-based fuel.

---

[*] *Corresponding author*. IMDEA Energy Institute, c/Tulipán s/n, 28933 Mostoles, Madrid, Spain. Tel.: +34 91 614 41 77; fax: +34 91 488 85 64.
E-mail address: fontina.petrakopoulou@imdea.org (F. Petrakopoulou).

doi:10.1016/j.ijhydene.2012.01.147

However, although the combustion of pure hydrogen produces only water vapor and heat, the processes used to obtain hydrogen generate harmful emissions. These emissions must be treated and removed.

The present paper is part of a study that compares different technologies for CO_2 capture under similar conditions. All CO_2 capture plants are based on the same reference power plant, making possible the comparison of their performance at the same size and structural characteristics. Here, two power plants that convert methane into hydrogen-based fuels are presented and evaluated. The first plant includes a hydrogen-separating methane steam reforming membrane (MSR plant) [11–13], and the second, an autothermal reformer (ATR plant), where complete and partial oxidation of methane take place [14,15]. The plants are analyzed using an exergetic analysis [16] and are compared to a reference plant that does not include CO_2 capture. Additionally, for a more complete overall evaluation of the pre-combustion technologies, the plants are briefly compared with plants that incorporate post-combustion and oxy-fuel capture technologies [10,17,18]. Using the results of the exergetic analysis we can improve the overall efficiency of the plant by decreasing the inefficiencies of its individual components. By increasing the efficiency of the overall plant, the fuel input required for the production of a given product output decreases, reducing the emissions per unit of output.

2. The power plants

2.1. *Reference plant*

The reference plant is a combined-cycle power plant with a three-pressure-level heat-recovery steam generator (HRSG). A simplified diagram of the plant is shown in Fig. 1. A detailed description of the operation of the plant and the results of its exergy-based examinations can be found in [17,19,20].

2.2. *Plant using a methane steam reforming membrane with hydrogen separation (MSR plant)*

A simplified diagram of the plant is shown in Fig. 2, while its detailed structure can be seen in Fig. A.1. The hydrogen-separating membrane (Fig. 3) uses thermal energy from the flue gases of the plant to reform the methane entering the plant into CO_2, H_2 and H_2O. To simulate a best-case scenario, we assume a sequence of H_2 separation steps according to Jordal et al. [6], until we achieve the separation of 99.7% of the generated hydrogen in the membrane. The hydrogen is then swept by intermediate-pressure steam at 17 bar and led to the combustion chamber (CC) of the plant. The remaining gases (CO_2 and H_2O) exit the membrane and the CO_2 is captured after water condensation [5,6].

Initially, methane is mixed with steam (mass ratio 1:4) extracted from a high-pressure steam turbine (HPST) at 50 bar. The mixture is preheated in a natural gas preheater (NGPH) and led to the feed side of the reactor of the plant at a temperature of 600 °C. The reforming process is a strongly endothermic reaction, for which thermal energy is provided by the combustion products of the plant. After the reforming process, the exothermic shifting reaction follows. 99.8% of the incoming methane is reformed and 99% of the produced CO is shifted [4]. The hydrogen formed is continuously transported through the membrane, which separates the feed and permeate sides of the reactor, and is swept from the permeate side of the reactor by intermediate-pressure (IP) steam. To have sufficient energy for the reforming process of the reactor and for the HRSG of the plant, a supplementary firing (duct burner, DB) is added after the CC, increasing the temperature of the combustion gases to 960 °C [6].

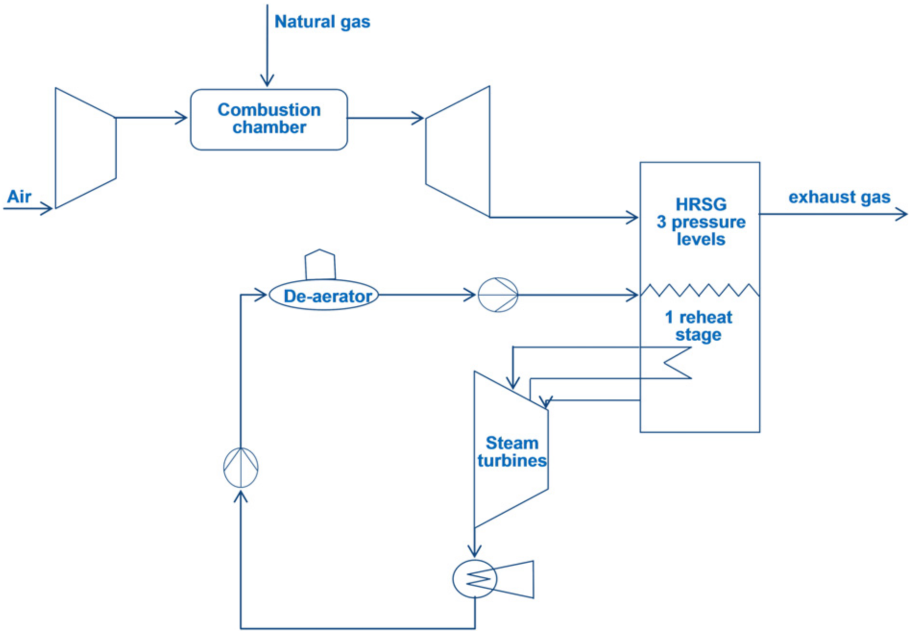

Fig. 1 – Simplified diagram of the reference plant [10].

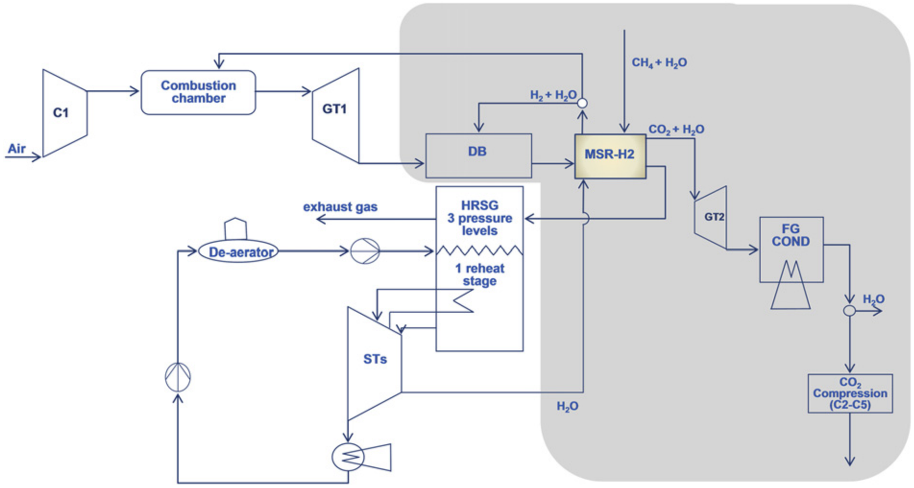

Fig. 2 – Simplified diagram of the MSR plant (grey box highlights differences with the reference plant) [10].

2.3. *Plant using an autothermal reformer (ATR plant)*

In the ATR plant, both partial and complete combustion give the necessary heat for reforming the methane. In more detail, an ATR is an adiabatic vessel, where the catalyst is placed, and the three main reactions occur (shown on the right side of Fig. 4) [8]. The first two reactions represent the steam reforming and water shift reactions, whereas the third reaction is a combination of the total combustion that usually takes place in an oxygen-rich environment and the catalytic partial oxidation (CPO). CPO has received considerable attention in recent years because of its close to 100% CH_4 conversion and its high H_2 yields. The amount of methane converted in the reaction depends on the steam to carbon (S/C) and the carbon to oxygen (C/O) ratios. As a result of the work of Luwei Chen et al. (2007), an optimal C/O ratio of 2 was set for an ATR operating at 15 bar and 850 °C, allowing *x* and *y* of the CPO to be set to 1.2 and 0.9, respectively, as shown in Equation (1). The S/C ratio was also set to 2.

$$CH_4 + 0.95O_2 \rightleftharpoons 1.2H_2 + 0.9CO + 0.8H_2O + 0.1CO_2 \qquad (1)$$

Air is supplied to the ATR by compressor extraction (Fig. 4 and Fig. A.2). The equilibrium temperature of the mixed stream is approximately 380 °C, a temperature too low for the ATR that operates at 850 °C. For this reason, the ATR outlet stream, a mixture of the combustion and the reforming products that exits the unit at 850 °C is used to preheat the ATR inlet stream to 640 °C in the NGPH of the plant. After the ATR, the gas is sent to the two shift reactors of the plant, where the produced CO is converted to CO_2 and H_2O. The simulation of the shift reactors has been realized by calculating the equilibrium constants of the reaction, which are controlled by the equilibrium temperature. Because of the high percentage of nitrogen in the gas, chemical absorption is used to capture the produced CO_2. Therefore, the gas is cooled to 60 °C and sent to a chemical absorption unit (CAU). The necessary thermal energy for the regeneration of the chemical solvent (monoethanolamine, MEA) is provided from a low-pressure steam extraction. After the CAU, the captured CO_2 is led to the compression unit, while the hydrogen-rich gas (fuel) is sent to the CC.

Fiaschi and Tapinassi [15] have performed research on the integration of an autothermal reformer into a gas turbine system. However, the plants they examined do not include bottoming steam cycles. In the same work, the required heat demand of the endothermic steam reforming is provided by thermal energy of the flue gases, while CO_2 separation is performed with DEA and MDEA. In an attempt to decrease the size of the syngas treatment section and to facilitate the CO_2 separation, an air membrane-ATR that operates with an oxygen separating membrane has been examined in [21]. However, the plant also resulted in a relatively high energy penalty of approximately 10 percentage points.

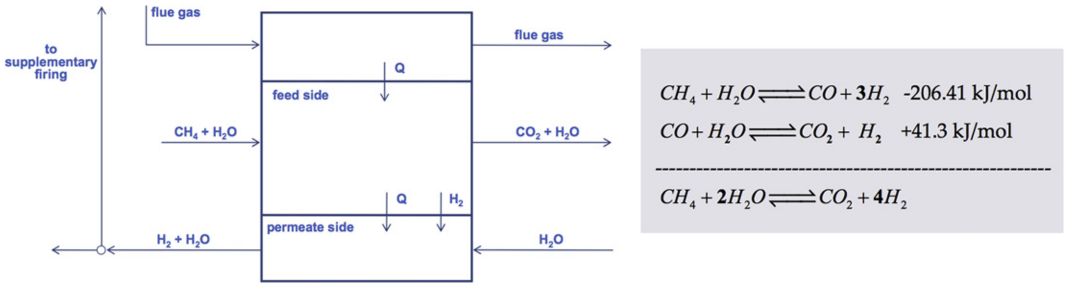

Fig. 3 – Configuration of the MSR reactor and the chemical reactions [10].

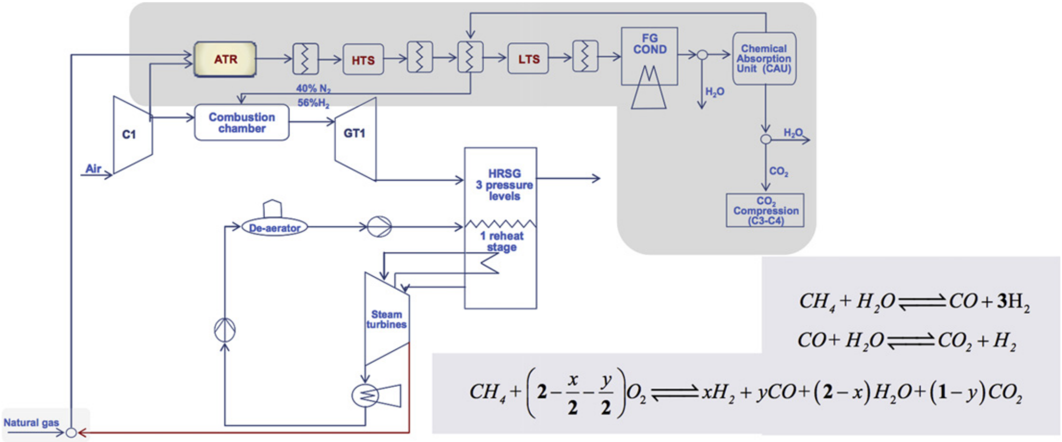

$$CH_4 + H_2O \rightleftharpoons CO + 3H_2$$

$$CO + H_2O \rightleftharpoons CO_2 + H_2$$

$$CH_4 + \left(2 - \frac{x}{2} - \frac{y}{2}\right)O_2 \rightleftharpoons xH_2 + yCO + (2-x)H_2O + (1-y)CO_2$$

Fig. 4 – Simplified diagram of the plant with an ATR (grey box highlights differences with the reference plant).

3. Methodology

The evaluation of the plants has been performed at the component level using an exergetic analysis [16,22,23]. The rate of exergy of the product of component k, $\dot{E}_{p,k}$, is the exergy of the desired output resulting from the operation of the component, while the rate of exergy of the fuel of the same component, $\dot{E}_{F,k}$, is the expense in exergetic resources for the generation of the desired output. The rate of exergy destruction within component k, $\dot{E}_{D,k}$, is calculated as the difference between its rate of fuel and product exergy ($\dot{E}_{D,k} = \dot{E}_{F,k} - \dot{E}_{P,k}$). General guidelines for defining exergetic efficiencies have been proposed by Lazzaretto and Tsatsaronis (2006) and have also been used here. Definitions of exergy of the fuel and product and efficiencies for selected components of the MSR plant (based on Fig. A.1) are shown in Table 1. Similar definitions have been followed for the ATR plant as well.

Important variables of the exergetic analysis are the exergy destruction ratio, y_D, and the exergy loss ratio, y_L. The latter is only defined for the overall system. The exergy destruction ratio can be used to compare dissimilar components of the same system, while the total exergy destruction and exergy loss ratios can be used to compare different thermodynamic systems.

Table 1 – Definition of exergy of the product and fuel and exergetic efficiency of selected components of the MSR plant.

	$\dot{E}_{P,k}$	$\dot{E}_{F,k}$	ε_k
C1	$\dot{E}_2 - \dot{E}_1$	$\dot{W}$	$\frac{\dot{W}}{\dot{E}_2 - \dot{E}_1}$
CC	$\dot{E}_4 - \dot{E}_2$	$\dot{E}_{49}$	$\frac{\dot{E}_{49}}{\dot{E}_4 - \dot{E}_2}$
GT1	$\dot{W}$	$\dot{E}_4 - \dot{E}_5$	$\frac{\dot{W}}{\dot{E}_4 - \dot{E}_5}$
RH	$\dot{E}_{27} - \dot{E}_{26}$	$\dot{E}_8 - \dot{E}_9$	$\frac{\dot{E}_{27} - \dot{E}_{26}}{\dot{E}_8 - \dot{E}_9}$
HPST	$\dot{W}$	$\dot{E}_{39} - \dot{E}_{40} - \dot{E}_{48}$	$\frac{\dot{W}}{\dot{E}_{39} - \dot{E}_{40} - \dot{E}_{48}}$
COND	–	$\dot{E}_{43} - \dot{E}_{46}$	–

With an exergetic analysis the main sources of thermodynamic irreversibilities within a plant are identified. If necessary, modifications to the plant can then be applied, in order to reduce these inefficiencies. Since the adoption and/or the development of systems are mainly driven by economics, the thermodynamically optimal design can be used as the starting point for cost reduction and eventually cost minimization.

4. Results and discussion

The overall results of the exergetic analysis for the reference and the two pre-combustion plants are shown in Table 1. Detailed stream and component data of the plants with CO_2 capture can be found in Tables A.1 and A.2. All examined plants are provided with the same amount of natural gas and the small differences in the exergy of the fuel for the total plant ($\dot{E}_{F,tot}$) are associated with slightly different amounts of air required in each plant. The derived rate of the total exergy of the product ($\dot{E}_{P,tot}$) depends on the individual operating characteristics of the plants and the requirements of the respective CO_2 capture technology.

The reference plant performs with an exergetic efficiency of 56.5%. Both of the plants that incorporate CO_2 capture present high efficiency penalties. The ATR plant performs better than the MSR plant, but it still suffers a penalty of 10 percentage points, relative to the reference plant. This result agrees with the work presented by Romano et al. [24] and Ertesvag et al. [14]. In [24], various software was used for the simulation of the different parts of the power plant, while MDEA is used for the capture of the CO_2. The relatively lower penalty calculated there (8 percentage points when compared with a reference plant) is mainly associated with the lower assumed energy penalty of the CO_2 capture (0.99 MJ/kg CO_2 while here we assumed an MEA regeneration penalty of 1.1 MJ/kg CO_2) (Table 2).

With respect to the ATR plant, in the MSR plant the gas turbine (GT) system and the steam turbine (ST) generate less power, while more power is required by the CO_2 compressors (C2-C5 in Fig. A.2). Thus, the overall net power of the MSR plant and its efficiency are found to be lower than those of the ATR plant.

Table 2 – Selected results of the exergetic analysis.

	Ref. plant	ATR plant	MSR plant
ε_{tot} (%)	56.5	46.5	45.8
$\dot{E}_{P,tot}$(MW)	412.5	339.8	334.6
$\dot{E}_{D,tot}$ (MW)	300.4	358.1	338.7
$\dot{E}_{L,tot}$ (MW)	17.6	32.7	57.3
$y_{D,tot}$ (%)	41.1	49.0	46.4

To obtain an idea of the overall performance of the considered plants, we compare them with other CO_2 capture technologies. The most widely known and easily applicable method to capture CO_2 from power plants is post-combustion capture with chemical absorption using monoethanolamine (MEA plant) [25]. The results of the considered MEA plant can be found in [26]. When compared to the reference plant, the post-combustion plant shows an efficiency penalty of 8 percentage points, thus performing more efficiently than the ATR plant by 2 percentage points. Additionally, if we compare the ATR and MSR plants to oxy-fuel alternatives [10,27], their efficiency penalties appear even more severe. The justification of these results for the ATR plant is that it combines two costly CO_2 capture methods: chemical absorption and fuel de-carbonization. Chemical absorption requires large amounts of thermal energy, while the de-carbonization process includes a, strongly endothermic, reforming reaction that is fueled by supplementary fuel burning. The low efficiency of the MSR plant can be primarily explained by its high rate of exergy loss (7.8% of the $\dot{E}_{F,tot}$), which is associated with the high exergy of the flue gases exhausted to the environment ($\dot{E}_{L,tot}$).

As can be seen from the results of the exergetic analysis (Table A.2), the combustion chambers are responsible for the highest exergy destruction among the plant components. Apart from the dominant influence of the combustion chambers on the operation of the plants, other components also appear to play significant roles. In the ATR plant, the second highest exergy destruction is found within the ATR, followed by the CAU. Specifically, within the ATR and the CAU, 7% and 4% of the plant's $\dot{E}_{F,tot}$ is destroyed. In the DB of the MSR plant approximately 12% of the exergy of the fuel is destroyed, while in the MSR reactor approximately 1%. The compressor and the expander of the main GT system (C1 and GT1) also present relatively high exergy destruction. When comparing the pressure levels in each HRSG of the plants, the high-pressure level (HPSH, HPEV and HPEC) is found to be the most important part, followed by the low-pressure level (LPSH, LPEV and LPEC). Lastly, in the MSR plant, the CO_2 compression unit (C2–C5, COOL1-COOL4, FG COND) is responsible for destroying approximately 3% of the $\dot{E}_{F,tot}$.

Using the results of an exergetic analysis, we can improve the effectiveness of energy conversion systems by changing the design and operation of components with a high overall influence. By applying measures to decrease a component's exergy destruction, we can eventually decrease the irreversibilities of the overall structure. Improvement steps based on the findings of this study will be realized and reported in future work by the authors.

Although the simulation of the presented plants is based on the same reference plant, when evaluating the overall performance and risks associated with different technologies, some additional parameters must be accounted for as well. These parameters differ among the plants and depend on technology, structural complexity and operation. An important factor is that the plants presented here employ already commercially available technology, whereas for example oxy-fuel plants, include components not yet available on the market and are therefore associated with higher uncertainty. Components under development should satisfy safety constraints and must be examined under realistic conditions. Safety and maintainability are important issues when CCS technologies are considered. Additionally, the higher the complexity of a plant, the higher its operating challenges. Structural subsystems, such as recirculation gas routes, make the start-up, operation and maintenance of a plant more complex. Another evaluation criterion could be the quantity of resources (e.g., water) required for the operation of a plant. In the plants examined here, the need for a constant additional water supply is dominant, due to the water leaving the Rankine cycle and used in different parts of the plants. The water condensed in plant components, for example during CO_2 compression, could be re-used in the Rankine cycle after appropriate treatment. Also, in both plants steam generated in the Rankine cycle is mixed with the incoming natural gas. In the ATR plant, steam is also used in the chemical absorption unit, while in the MSR plant steam is used as the sweep gas of the membrane. This additional water demand requires specific conditions and extra environmental consideration. Lastly, additional safety considerations are needed to sequester the captured CO_2 and to examine all possible options thoroughly before large-scale facilities for CO_2 capture are established.

5. Conclusions

In this paper, two power plants (one with a hydrogen-separating steam reforming membrane and one with an autothermal reformer) with CO_2 capture have been compared and evaluated from a thermodynamic viewpoint. The plants perform pre-combustion carbon capture by converting the carbon-based fuel (methane) into a hydrogen-based fuel that is then combusted in the reactors of the plants. The structure and main operating characteristics of the plants were based on a reference plant that does not include CO_2 capture. The two pre-combustion plants were evaluated relative to both the reference plant and other proposed CO_2 capture technologies.

The plants were examined using an exergetic analysis. It was found that the largest part of exergy destruction is present within the combustion chambers of the plants, while high irreversibilities are also noted in the reforming components. Using the results of the presented analysis, improved structures of the plants can be obtained through the minimization of the exergy destruction within individual plant components of high importance. When compared to the reference plant, the plants with CO_2 capture perform thermodynamically poorly with a minimum efficiency penalty of approximately 10 percentage points, calculated for the plant that includes the autothermal reformer. The plant with the methane steam reforming membrane was found to have an additional penalty of 0.8 points. Lastly, when compared to power plants that incorporate other capture alternatives, the considered plants perform significantly less efficiently. Nevertheless, steps for decreasing the exergy destruction of the plants will be performed and presented in future publications, in order to reveal the potential for improvement of these carbon capture technologies.

Acknowledgments

This research was funded by the European Commission's Marie Curie 6th Framework Programme as part of the Research Training Network, INSPIRE, MRTN-CT-2005-019296.

The authors would like to thank Evonik Energy Systems GmbH for their support with the software Ebsilon Professional.

Nomenclature

$\dot{E}$	Exergy rate, MW
$\dot{m}$	Mass flow, kg/s
p	Pressure, bar
T	Temperature °C
y	Exergy destruction ratio, %
$\dot{Y}$	Component-related environmental impact, Pts/h

Subscripts

D	Exergy destruction
F	Fuel (exergy)
P	Product (exergy)
i,j	Stream
k	Component
L	Loss

Greek symbols

ε	Exergetic efficiency, %

Abbreviations

APH	Air preheater
ATR	Autothermal reformer
C (1–6)	Compressor
CAU	Chemical absorption unit
CC	Combustion chamber
CCS	Carbon capture and storage
COND	Condenser
COOL	Cooler
CPO	Catalytic partial oxidation
CT	Cooling tower
DB	Duct burner
EC	Economizer
EV	Evaporator
FG	Flue gas
GT	Gas turbine
HP, IP, LP	High pressure, intermediate pressure, low pressure
HRSG	Heat recovery steam generator
HX	Heat exchanger
IGCC	Integrated gasification combined-cycle
LCA	Life cycle assessment
M, Mix	Mixer
MEA	Monoethanolamine
MSR	Methane steam reformer
MUW	Make-up water
NG	Natural gas
P	Pump
PF	Pollutant formation
PH	Preheater
RH	Reheater
SH	Superheater
ST	Steam turbine
WPH	Water preheater

Appendix

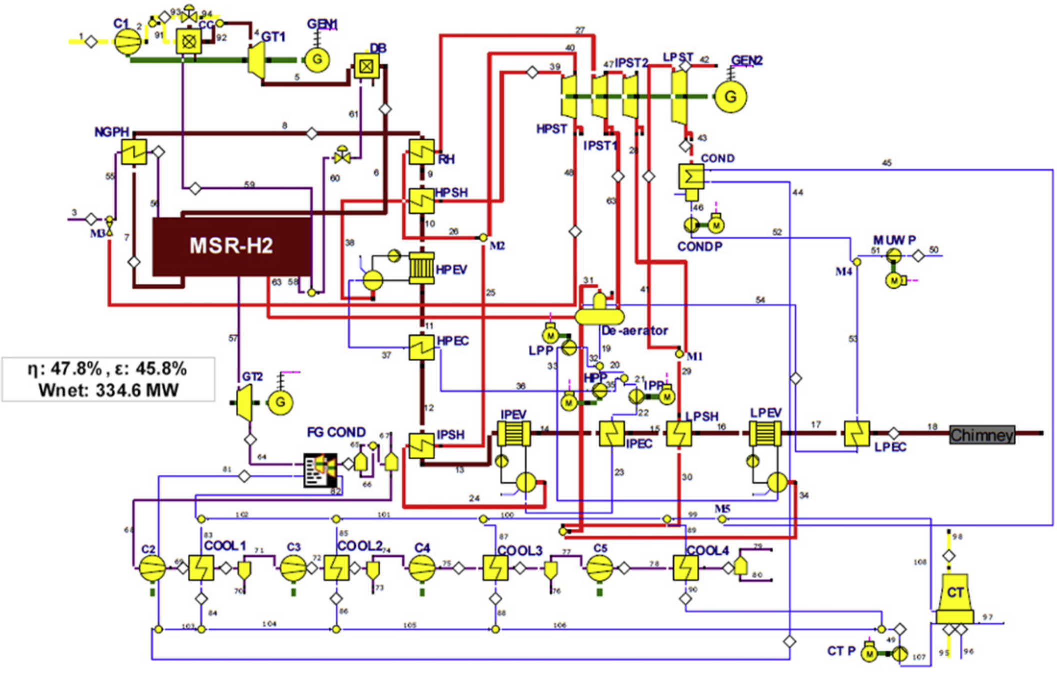

Fig. A.1 – Structure of the MSR plant. The component abbreviations are explained in the nomenclature of the paper.

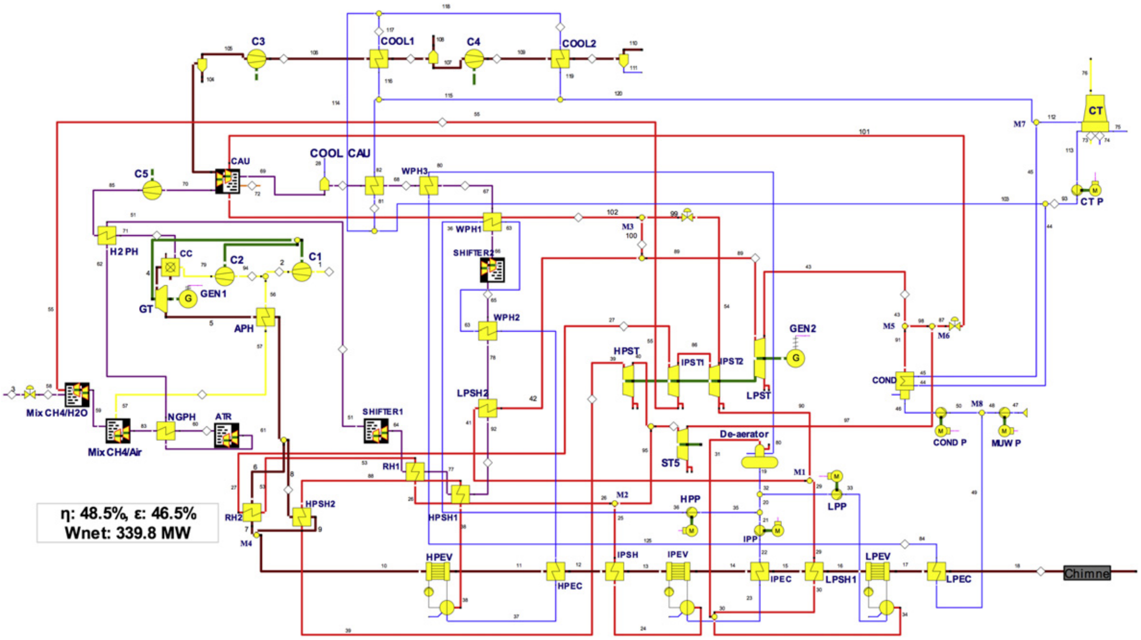

Fig. A.2 – Structure of the plant with an autothermal reformer (ATR plant). The component abbreviations are explained in the nomenclature of the paper.

Table A.1 – Results at the component level for the ATR plant (left) and MSR plant (right).

Component, k	$\dot{E}_{F,k}$ (MW)	$\dot{E}_{P,k}$ (MW)	$\dot{E}_{D,k}$ (MW)	ε_k (%)	$y_{D,k}$ (%)	Component, k	$\dot{E}_{F,k}$ (MW)	$\dot{E}_{P,k}$ (MW)	$\dot{E}_{D,k}$ (MW)	ε_k (%)	$y_{D,k}$ (%)
C1	221.95	211.43	10.53	95.3	1.44	C1	206.31	196.73	9.58	95.4	1.31
CC	659.64	502.80	156.84	76.2	21.47	CC	598.70	455.59	143.11	76.1	19.59
GT1	519.91	500.85	19.06	96.3	2.61	DB	338.16	252.94	85.23	74.8	11.66
HPSH1	2.37	2.06	0.31	86.9	0.04	GT1	481.89	463.51	18.37	96.2	2.51
HPSH2	26.00	23.38	2.62	89.9	0.36	GT2	54.18	50.81	3.37	93.8	0.46
HPEV	36.90	32.76	4.14	88.8	0.57	RH	8.28	7.21	1.07	87.1	0.15
HPEC	10.69	9.40	1.29	87.9	0.18	HPSH	36.79	32.41	4.38	88.1	0.60
RH1	11.37	10.65	0.72	93.7	0.10	HPEV	47.13	40.95	6.17	86.9	0.84
RH2	8.76	7.95	0.81	90.8	0.11	HPEC	32.45	25.58	6.86	78.8	0.94
IPSH	5.51	4.72	0.79	85.6	0.11	IPSH	0.70	0.59	0.11	83.7	0.02
IPEV	30.37	26.75	3.62	88.1	0.50	IPEV	10.47	9.89	0.59	94.4	0.08
IPEC	6.89	5.75	1.14	83.5	0.16	IPEC	3.45	2.84	0.62	82.2	0.08
LPSH1	1.54	1.14	0.40	74.1	0.05	LPSH	3.17	2.40	0.77	75.7	0.11
LPSH2	3.37	2.86	0.52	84.7	0.07	LPEV	27.16	21.11	6.05	77.7	0.83
LPEV	19.39	15.73	3.66	81.1	0.50	LPEC	13.93	9.33	4.60	67.0	0.63
LPEC	13.01	8.44	4.57	64.9	0.63	NGPH	32.62	28.56	4.06	87.6	0.56
NGPH	34.36	30.19	4.17	87.9	0.57	HPST	17.71	16.64	1.08	93.9	0.15
H2 PH	32.61	25.32	7.30	77.6	1.00	IPST1	8.22	7.78	0.45	94.6	0.06
APH	9.38	5.91	3.47	63.0	0.47	IPST2	0.29	0.27	0.02	93.6	0.00
WPH1	3.05	2.69	0.36	88.1	0.05	LPST	22.33	19.29	3.03	86.4	0.42
WPH2	10.38	9.53	0.86	91.7	0.12	MSR-H2	180.20	171.88	8.32	95.4	1.14
WPH3	1.26	1.10	0.16	87.2	0.02	COND P	0.02	0.01	0.01	68.5	0.00
HPST	19.56	18.30	1.26	93.6	0.17	LPP	0.00	0.00	0.00	69.4	0.00
IPST1	19.98	18.91	1.07	94.6	0.15	HPP	1.14	0.98	0.16	85.7	0.02
IPST2	15.88	14.64	1.24	92.2	0.17	IPP	0.12	0.08	0.03	70.7	0.00
LPST	23.85	20.61	3.24	86.4	0.44	MUW P	0.03	0.02	0.01	77.0	0.00
ST5	11.30	9.91	1.39	87.7	0.19	C2	3.84	3.19	0.64	83.2	0.09
ATR	809.32	–	51.81	–	7.09	C3	4.06	3.37	0.69	83.0	0.09
SHIFTER1	690.54	–	3.43	–	0.47	C4	4.04	3.33	0.71	82.4	0.10
SHIFTER2	659.61	–	0.63	–	0.09	C5	4.10	3.34	0.76	81.4	0.10
CAU	33.54	–	29.95	–	4.10	De-aerator	0.51	0.49	0.02	95.6	0.00
COND P	0.04	0.03	0.01	77.5	0.00	M1	0.02	0.02	0.00	96.1	0.00
HPP	1.05	0.89	0.17	84.3	0.02	M2	1.17	1.07	0.10	91.5	0.01
IPP	0.18	0.14	0.04	77.8	0.01	M3	569.88	565.03	4.85	99.1	0.66

Table A.1 – (*continued*)

Component, k	$\dot{E}_{F,k}$ (MW)	$\dot{E}_{P,k}$ (MW)	$\dot{E}_{D,k}$ (MW)	ε_k (%)	$y_{D,k}$ (%)	Component, k	$\dot{E}_{F,k}$ (MW)	$\dot{E}_{P,k}$ (MW)	$\dot{E}_{D,k}$ (MW)	ε_k (%)	$y_{D,k}$ (%)
LPP	0.05	0.01	0.03	28.9	0.00	M4	0.06	0.01	0.05	22.9	0.01
MUW P	0.01	0.01	0.00	68.0	0.00	M5	0.53	0.45	0.08	85.1	0.01
C2	10.21	9.84	0.37	96.4	0.05	FG COND	16.69	–	15.06	–	2.06
C3	2.70	2.21	0.48	82.0	0.07	COOL1	0.68	–	0.60	–	0.08
C4	2.87	2.33	0.54	81.2	0.07	COOL2	0.94	–	0.85	–	0.12
C5	4.34	3.58	0.76	82.4	0.10	COOL3	0.89	–	0.80	–	0.11
De-aerator	0.65	0.62	0.03	95.7	0.00	COOL4	0.92	–	0.83	–	0.11
M1	0.17	0.16	0.01	95.9	0.00	COND	4.02	–	2.99	–	0.41
M2	0.23	0.23	0.00	99.4	0.00	CT	2.93	–	1.62	–	0.22
M4	1.79	1.78	0.01	99.2	0.00	*Total*	*730.63*	*334.64*	*338.70*	*45.8*	*46.36*
M5	2.11	2.11	0.00	100.0	0.00	*Exergy loss*	*57.29*				
M6	1.01	0.95	0.06	94.1	0.01						
M7	0.31	0.27	0.03	88.9	0.00						
M8	0.08	0.04	0.05	43.0	0.01						
Mix CH_4/Air	428.31	419.98	8.33	98.1	1.14						
Mix CH_4/H_2O	507.54	500.94	6.60	98.7	0.90						
COOL CAU	13.71	–	12.63	–	1.73						
COOL1	0.73	–	0.67	–	0.09						
COOL2	0.62	–	0.56	–	0.08						
COND	5.17	–	3.85	–	0.53						
CT	2.50	–	1.48	–	0.20						
Total	*730.62*	*339.81*	*358.06*	*46.5*	*49.01*						
Exergy loss	*32.75*										

Table A.2. – Results at the stream level for the ATR plant (left) and MSR plant (right).

Stream, j	$\dot{m}_j$ (kg/s)	T_j (°C)	p_j (bar)	$\dot{E}_{PH,j}$ (MW)	$\dot{E}_{CH,j}$ (MW)	$\dot{E}_{tot,j}$ (MW)	$\dot{m}_j$ (kg/s)	T_j (°C)	p_j (bar)	$\dot{E}_{PH,j}$ (MW)	$\dot{E}_{CH,j}$ (MW)	$\dot{E}_{tot,j}$ (MW)
1	590.89	15.00	1.01	0.00	0.92	0.92	523.00	15.00	1.01	0.00	0.81	0.81
2	590.89	375.07	15.46	211.43	0.92	212.35	523.00	392.51	17.00	196.73	0.81	197.54
3	14.00	15.00	50.00	8.15	721.47	729.62	14.00	15.00	50.00	8.15	721.47	729.62
4	588.87	1250.87	16.49	701.33	1.78	703.11	542.30	1230.15	16.49	652.06	1.07	653.13
5	588.87	577.02	1.11	181.42	1.78	183.19	542.30	567.08	1.11	170.17	1.07	171.25
6	178.87	562.53	1.06	52.24	0.54	52.78	553.20	994.77	1.10	422.50	1.69	424.18
7	178.87	498.89	1.05	43.48	0.54	44.02	553.20	674.76	1.06	242.30	1.69	243.98
8	410.00	562.53	1.06	119.78	1.24	121.02	553.20	609.47	1.06	209.68	1.69	211.37
9	410.00	479.33	1.05	93.78	1.24	95.02	553.20	592.38	1.06	201.40	1.69	203.09
10	588.87	485.28	1.05	137.25	1.78	139.03	553.20	513.25	1.05	164.61	1.69	166.30
11	588.87	395.77	1.05	100.35	1.78	102.13	553.20	401.68	1.05	117.48	1.69	119.17
12	588.87	367.81	1.05	89.66	1.78	91.43	553.20	314.01	1.04	85.04	1.69	86.72
13	588.87	352.91	1.05	84.14	1.78	85.92	553.20	311.97	1.04	84.34	1.69	86.02
14	588.87	263.09	1.04	53.77	1.78	55.55	553.20	280.43	1.04	73.86	1.69	75.55
15	588.87	240.05	1.04	46.88	1.78	48.66	553.20	269.55	1.04	70.41	1.69	72.09
16	588.87	234.70	1.04	45.34	1.78	47.11	553.20	259.32	1.04	67.23	1.69	68.92
17	588.87	158.26	1.03	25.95	1.78	27.72	553.20	156.38	1.03	40.07	1.69	41.76
18	588.87	83.81	1.03	12.94	1.78	14.72	553.20	72.68	1.03	26.14	1.69	27.82
19	112.53	142.17	3.84	10.41	0.28	10.69	111.13	139.81	3.60	9.93	0.28	10.21
20	89.32	142.17	3.84	8.26	0.22	8.48	79.81	139.81	3.60	7.13	0.20	7.33
21	34.11	142.17	3.84	3.15	0.09	3.24	12.89	139.81	3.60	1.15	0.03	1.18
22	34.11	142.74	39.68	3.30	0.09	3.38	12.89	140.86	57.12	1.24	0.03	1.27
23	34.11	242.09	38.49	9.05	0.09	9.13	12.89	264.43	55.40	4.07	0.03	4.11
24	34.11	248.09	38.49	35.80	0.09	35.89	12.89	270.43	55.40	13.96	0.03	13.99
25	34.11	347.81	36.57	40.52	0.09	40.61	12.89	294.01	52.63	14.55	0.03	14.58
26	78.85	352.99	36.57	94.21	0.20	94.41	23.81	347.74	52.63	28.84	0.06	28.90
27	78.85	532.53	33.00	112.81	0.20	113.01	23.81	559.47	50.00	36.05	0.06	36.10
28	17.69	60.00	13.20	0.26	0.04	0.30	0.83	217.70	4.10	0.67	0.00	0.68
29	22.26	220.05	4.32	18.30	0.06	18.35	30.57	249.55	4.10	25.74	0.08	25.82
30	22.26	148.26	4.54	17.16	0.06	17.21	30.57	146.37	4.32	23.34	0.08	23.42

(*continued on next page*)

Table A.2. – (*continued*)

Stream, j	$\dot{m}_j$ (kg/s)	T_j ($^{\circ}$C)	p_j (bar)	$\dot{E}_{PH,j}$ (MW)	$\dot{E}_{CH,j}$ (MW)	$\dot{E}_{tot,j}$ (MW)	$\dot{m}_j$ (kg/s)	T_j ($^{\circ}$C)	p_j (bar)	$\dot{E}_{PH,j}$ (MW)	$\dot{E}_{CH,j}$ (MW)	$\dot{E}_{tot,j}$ (MW)
31	0.95	148.26	4.54	0.74	0.00	0.74	0.75	146.37	4.32	0.58	0.00	0.58
32	23.21	142.17	3.84	2.15	0.06	2.20	31.32	139.81	3.60	2.80	0.08	2.88
33	23.21	142.56	4.54	2.16	0.06	2.22	31.32	139.82	4.32	2.80	0.08	2.88
34	23.21	148.26	4.54	17.89	0.06	17.95	31.32	146.37	4.32	23.92	0.08	24.00
35	55.21	142.17	3.84	5.11	0.14	5.24	66.92	139.81	3.60	5.98	0.17	6.15
36	55.21	144.16	146.05	5.99	0.14	6.13	66.92	141.54	134.56	6.96	0.17	7.13
37	55.21	329.19	137.40	27.61	0.14	27.74	66.92	325.17	130.53	32.54	0.17	32.71
38	55.21	335.19	137.40	60.37	0.14	60.51	66.92	331.17	130.53	73.50	0.17	73.67
39	55.21	542.53	124.00	85.81	0.14	85.94	66.92	559.38	124.00	105.91	0.17	106.08
40	55.21	356.97	36.57	66.25	0.14	66.39	10.92	422.41	52.63	14.39	0.03	14.41
41	30.28	228.43	4.32	25.12	0.08	25.19	31.40	248.71	4.10	26.42	0.08	26.50
42	30.28	331.00	4.10	27.97	0.08	28.05	0.00	32.88	0.05	0.00	0.00	0.00
43	30.28	32.88	0.05	4.12	0.08	4.20	31.40	32.88	0.05	4.09	0.08	4.17
44	3078.21	16.00	1.37	0.13	7.69	7.82	2394.26	16.00	1.37	0.10	5.98	6.08
45	3078.21	22.88	1.33	1.46	7.69	9.15	2394.26	22.88	1.33	1.14	5.98	7.12
46	80.52	32.88	0.05	0.17	0.20	0.37	31.40	32.88	0.05	0.07	0.08	0.15
47	31.05	15.00	1.01	0.00	0.08	0.08	0.83	392.96	17.00	0.97	0.00	0.97
48	31.05	15.02	4.08	0.01	0.08	0.09	56.00	422.41	52.63	73.81	0.14	73.95
49	111.57	27.92	4.08	0.17	0.28	0.44	4731.69	16.00	1.37	0.21	11.82	12.02
50	80.52	32.90	4.08	0.20	0.20	0.41	78.98	15.00	1.01	0.00	0.20	0.20
51	105.94	350.00	14.06	66.40	624.13	690.54	78.98	15.01	3.71	0.02	0.20	0.22
52	55.21	268.18	141.65	18.21	0.14	18.34	31.40	32.90	3.71	0.08	0.08	0.16
53	78.85	457.45	34.74	104.86	0.20	105.06	110.38	20.10	3.71	0.05	0.28	0.33
54	39.77	251.79	4.32	33.83	0.10	33.93	110.38	136.38	3.60	9.38	0.28	9.65
55	31.05	411.52	15.00	36.56	0.08	36.64	70.00	321.58	50.00	77.15	721.58	798.72
56	60.89	375.07	15.46	21.79	0.09	21.88	70.00	600.00	49.98	105.71	721.58	827.28
57	60.89	530.00	14.69	27.70	0.09	27.79	62.78	816.97	47.98	70.90	18.31	89.22
58	14.00	15.00	15.00	5.63	721.47	727.11	30.20	684.06	17.00	88.36	848.50	936.86
59	45.05	297.03	15.00	38.14	721.51	759.66	19.30	684.06	17.00	56.47	542.23	598.70
60	105.94	640.00	14.67	92.02	717.30	809.32	10.90	684.06	17.00	31.90	306.27	338.16
61	105.94	850.00	14.09	133.33	624.18	757.51	10.90	684.06	1.11	20.42	306.27	326.68
62	105.94	619.43	14.07	99.01	624.13	723.15	70.00	600.00	47.98	112.27	861.61	973.88
63	55.21	178.15	141.67	8.68	0.14	8.82	22.98	392.96	17.00	26.85	0.06	26.91
64	105.94	470.24	13.63	76.00	611.10	687.10	62.78	288.45	1.02	16.73	18.31	35.04
65	105.94	200.00	13.62	48.51	611.10	659.61	24.02	25.00	1.01	0.02	0.06	0.08
66	105.94	212.43	13.21	48.67	610.31	658.98	38.75	25.00	1.01	0.02	18.25	18.27
67	105.94	170.00	13.20	45.62	610.31	655.93	24.02	25.00	1.01	0.02	0.06	0.08
68	105.94	150.00	13.20	44.36	610.31	654.67	38.75	25.00	1.01	0.02	18.25	18.27
69	88.25	60.00	13.20	30.39	610.27	640.65	38.75	131.81	3.22	3.21	18.25	21.47
70	58.87	63.12	12.94	26.00	604.75	630.75	0.14	40.00	3.21	0.00	0.00	0.00
71	58.87	510.46	17.00	54.89	604.75	659.64	38.61	40.00	3.21	2.54	18.25	20.79
72	1088.22	31.23	14.00	3.42	2.72	6.14	38.61	151.95	10.22	5.91	18.25	24.16
73	3363.76	15.00	1.01	0.00	5.24	5.24	0.26	40.00	10.21	0.00	0.00	0.00
74	90.98	15.00	1.01	0.00	0.23	0.23	38.36	40.00	10.21	4.96	18.26	23.22
75	48.05	16.00	1.01	0.00	0.12	0.12	38.36	152.83	32.46	8.29	18.26	26.55
76	3406.68	23.64	1.01	1.46	4.89	6.36	0.08	40.00	32.45	0.00	0.00	0.00
77	105.94	372.99	13.63	64.63	611.10	675.73	38.28	40.00	32.45	7.39	18.27	25.66
78	105.94	318.25	13.62	58.89	611.10	669.99	38.28	154.99	103.09	10.73	18.27	29.00
79	530.00	392.88	17.00	199.48	0.82	200.31	0.03	30.00	103.09	0.00	0.00	0.00
80	111.57	137.89	3.84	9.70	0.28	9.98	38.25	30.00	103.09	9.80	18.28	28.08
81	1552.28	16.00	1.37	0.07	3.88	3.94	1932.57	16.00	1.37	0.08	4.83	4.91
82	1552.28	25.00	1.33	1.15	3.88	5.03	1932.57	26.00	1.33	1.72	4.83	6.54
83	105.94	385.00	14.69	61.83	717.30	779.12	86.75	26.00	1.33	0.08	0.22	0.29
84	111.57	130.00	3.96	8.60	0.28	8.88	86.75	16.00	1.37	0.00	0.22	0.22
85	58.87	97.75	17.08	29.57	604.75	634.32	111.06	26.00	1.33	0.10	0.28	0.38
86	47.80	411.52	15.00	56.27	0.12	56.39	111.06	16.00	1.37	0.00	0.28	0.28
87	39.77	20.09	0.05	0.00	0.10	0.10	100.23	26.00	1.33	0.09	0.25	0.34
88	55.21	338.32	130.53	62.43	0.14	62.56	100.23	16.00	1.37	0.00	0.25	0.25
89	30.28	331.00	4.10	27.97	0.08	28.05	106.82	26.00	1.33	0.09	0.27	0.36
90	8.03	251.79	4.32	6.83	0.02	6.85	106.82	16.00	1.37	0.00	0.27	0.27
91	80.52	32.88	0.05	5.34	0.20	5.54	419.00	392.51	17.00	157.61	0.65	158.26
92	105.94	351.00	13.63	62.26	611.10	673.37	438.30	1392.45	16.49	624.23	1.04	625.27
93	4805.37	16.00	1.37	0.21	12.00	12.21	104.00	392.51	17.00	39.12	0.16	39.28

Table A.2. – (*continued*)

Stream, j	$\dot{m}_j$ (kg/s)	T_j (°C)	p_j (bar)	$\dot{E}_{PH,j}$ (MW)	$\dot{E}_{CH,j}$ (MW)	$\dot{E}_{tot,j}$ (MW)	$\dot{m}_j$ (kg/s)	T_j (°C)	p_j (bar)	$\dot{E}_{PH,j}$ (MW)	$\dot{E}_{CH,j}$ (MW)	$\dot{E}_{tot,j}$ (MW)
94	530.00	375.07	15.46	189.64	0.82	190.47	104.00	392.51	16.49	38.86	0.16	39.02
95	44.74	356.97	36.57	53.69	0.11	53.80	3312.18	15.00	1.01	0.00	5.16	5.16
96	10.46	356.97	36.57	12.56	0.03	12.58	92.58	15.00	1.01	0.00	0.23	0.23
97	10.46	32.88	0.05	1.26	0.03	1.29	47.32	16.00	1.01	0.00	0.12	0.12
98	50.24	32.88	0.05	1.22	0.13	1.35	3357.45	24.42	1.01	1.75	4.83	6.57
99	39.77	251.43	4.10	33.56	0.10	33.66	2337.43	26.00	1.33	2.08	5.84	7.92
100	0.00	331.00	4.10	0.00	0.00	0.00	2230.61	26.00	1.33	1.98	5.57	7.55
101	39.77	20.00	4.10	0.02	0.10	0.12	2130.38	26.00	1.33	1.89	5.32	7.21
102	39.77	251.43	4.10	33.56	0.10	33.66	2019.32	26.00	1.33	1.79	5.04	6.84
103	1727.16	16.00	1.37	0.07	4.31	4.39	4326.83	16.00	1.37	0.19	10.81	11.00
104	0.13	57.11	12.94	0.00	0.00	0.00	4413.58	16.00	1.37	0.19	11.02	11.22
105	29.24	57.11	12.94	4.16	9.34	13.50	4524.64	16.00	1.37	0.20	11.30	11.50
106	29.24	155.75	34.60	6.37	9.34	15.71	4624.87	16.00	1.37	0.20	11.55	11.75
107	29.11	40.00	34.59	5.63	9.36	14.98	4731.69	16.00	1.01	0.03	11.82	11.85
108	0.14	40.00	34.59	0.00	0.00	0.00	4731.69	24.42	1.33	3.13	11.82	14.95
109	29.11	147.40	103.09	7.96	9.36	17.32					C1	206.31
110	29.09	30.00	103.09	7.33	9.36	16.69					ST1	16.67
111	0.02	30.00	103.09	0.00	0.00	0.00					ST2	7.80
112	4805.37	23.64	1.33	2.71	12.00	14.71					ST3	0.29
113	4805.37	16.00	1.01	0.03	12.00	12.04					ST4	19.33
114	174.88	16.00	1.37	0.01	0.44	0.44					COND P	0.02
115	1643.63	25.00	1.33	1.22	4.11	5.32					LPP	0.00
116	91.35	25.00	1.33	0.07	0.23	0.30					HPP	1.15
117	91.35	16.00	1.37	0.00	0.23	0.23					IPP	0.12
118	83.53	16.00	1.37	0.00	0.21	0.21					GT1	256.99
119	83.53	25.00	1.33	0.06	0.21	0.27					GT2	50.81
120	1727.16	25.00	1.33	1.28	4.31	5.60					MUW P	0.03
121					C1	221.95					C2	3.84
122					ST1	18.30					C3	4.06
123					ST2	18.91					C4	4.04
124					ST3	14.64					C5	4.10
125					ST4	20.61					tot	334.53
126					COND P	0.04						
127					LPP	0.05						
128					IPP	0.18						
129					HPP	1.05						
130					C2	10.21						
131					MUW P	0.01						
132					C5	4.34						
133					C3	2.70						
134					C4	2.87						
135					GT1	268.69						
136					ST5	9.91						
137					tot	339.81						

REFERENCES

[1] http://www.hydrogen.energy.gov/, U.S. Department Of Energy - Hydrogen and Fuel Cells Program, last accessed September 2011.

[2] Stiegel GJ, Ramezan M. Hydrogen from coal gasification: an economical pathway to a sustainable energy future. International Journal of Coal Geology 2006;65(3–4):173–90.

[3] Gnanapragasam NV, Reddy BV, Rosen MA. Hydrogen production from coal gasification for effective downstream CO_2 capture. International Journal of Hydrogen Energy 2010; 35(10):4933–43.

[4] Bottino A, Comite A, Capannelli G, Di Felice R, Pinacci P. Steam reforming of methane in equilibrium membrane reactors for integration in power cycles. Catalysis Today 2006;118:214–22.

[5] Johannessen E, Jordal K. Study of a H_2 separating membrane reactor for methane steam reforming at conditions relevant for power processes with CO_2 capture. Energy Conversion and Management 2005;46:1059–71.

[6] Jordal K, Bredesen R, Kvamsdal HM, Bolland O. Integration of H_2-separating membrane technology in gas turbine processes for CO_2 capture. Energy 2004;29:1269–78.

[7] Chen L, Hong Q, Lin J, Dautzenberg FM. Hydrogen production by coupled catalytic partial oxidation and steam methane reforming at elevated pressure and temperature. Journal of Power Sources 2007;164:803–8.

[8] Horn R, Williams KA, Degenstein NJ, Bitsch-Larsen A, Nogare DD, Tupy SA, et al. Methane catalytic partial oxidation on autothermal rh and pt foam catalysts: oxidation and reforming zones, transport effects, and approach to thermodynamic equilibrium. Journal of Catalysis 2007;249: 380–93.

[9] Clarke D, Debeljak B, Janeiro V de, Göttlicher G, Graham D, Kirkegaard N. CO_2 Capture and Storage, a Vgb report on the State of the Art. 2004.

[10] Petrakopoulou F. Comparative evaluation of power plants with CO_2 capture: thermodynamic, economic and environmental performance. Institut für Energietechnik; 2010.

[11] Harold MP, Naira B, Kolios G. Hydrogen generation in a pd membrane fuel processor: assessment of methanol-based reaction systems. Chemical Engineering Science 2003;58: 2551–71.

[12] Kvamsdal HM, Maurstad O, Jordal K, Bolland O. Benchmarking of gas-turbine cycles with CO_2 capture. n.d.

[13] Kvamsdal HM, Jordal K, Bolland O. A quantitative comparison of gas turbine cycles with CO_2 capture. Energy 2007;32:10–24.

[14] Ertesvag I, Kvamsdal HM, Bolland O. Exergy analysis of a gas-turbine combined-cycle power plant with precombustion CO_2 capture. Energy 2005;30(1):5–39.

[15] Fiaschi D, Tapinassi L. Exergy analysis of the recuperative autothermal reforming (r-atr) and recuperative reforming (r-ref) power cycles with CO_2 removal. Energy 2004;29:2003–24.

[16] Bejan A, Tsatsaronis G, Moran M. Thermal design and optimization. New York: Wiley-Interscience; 1995.

[17] Petrakopoulou F, Boyano A, Cabrera M, Tsatsaronis G. Exergy-based analyses of an advanced zero emission plant. International Journal of Low-Carbon Technologies 2010;5(4): 231–8.

[18] Petrakopoulou F, Boyano A, Cabrera M, Tsatsaronis G. Exergoeconomic and exergoenvironmental analyses of a combined cycle power plant with chemical looping technology. Int J Greenhouse Gas Control 2011;5(3):475–82.

[19] Petrakopoulou F, Tsatsaronis G, Morosuk T. Conventional exergetic and exergoeconomic analyses of a power plant with chemical looping combustion for CO_2 capture. International Journal of Thermodynamics 2010;13(3): 77–86.

[20] Petrakopoulou F, Tsatsaronis G, Morosuk T, Carassai A. Conventional and advanced exergetic analyses applied to a combined cycle power plant. Energy; 2011.

[21] Fiaschi D, Gamberi F, Bartlett M, Griffin T. The air membrane-atr integrated gas turbine power cycle: a method for producing electricity with low CO_2 emissions. Energy Conversion and Management 2005;46:2514–29.

[22] Lazzaretto A, Tsatsaronis G. Speco: a systematic and general methodology for calculating efficiencies and costs in thermal systems. Energy 2006;31:1257–89.

[23] Tsatsaronis G, Cziesla F. Thermoeconomics. In: Encyclopedia of physical science and technology. Academic Press; 2002. p. 659–80.

[24] Romano MC, Chiesa P, Lozza G. Pre-combustion CO_2 capture from natural gas power plants, with atr and mdea processes. Int J Greenhouse Gas Control 2010;4(5):785–97.

[25] Rubin ES, Rao AB. A technical, economic and environmental assessment of amine-based CO_2 capture technology for power plant greenhouse gas control; 2002.

[26] Petrakopoulou F, Tsatsaronis G, Morosuk T. Exergoeconomic analysis of an advanced zero emission plant. J Eng for Gas Turbines Power 2011;133(11):113001–12.

[27] Petrakopoulou F, Tsatsaronis G, Boyano A, Morosuk T. Exergoeconomic and exergoenvironmental evaluation of power plants including CO_2 capture. Chemical Engineering Research and Design 2010;89(9):1461–9.